JOURNAL OF NANO- AND ELECTRONIC PHYSICS *ЖУРНАЛ НАНО- ТА ЕЛЕКТРОННОЇ ФІЗИКИ*
Vol. **9** No 1, 01008(6pp) (2017) Том **9** № 1, 01008(6cc) (2017)

Effect of Severe Plastic Deformation on Shape Memory and Mechanical Properties of Nanostructured Cu-Zn-Al Alloy

M. Bagherpour[1,*], A. Shokouhfar[1], A. Zolriasatein[1,2], A. Farzaneh Bahelgerdy[1]

[1] *Advanced Materials and Nanotechnology Research Lab, Faculty of Materials Science and Engineering, K.N. Toosi University of Technology, 1999143344 Tehran, Iran*
[2] *Center for Nanotechnology Development, Niroo Research Institute (NRI), 1468617151 Tehran, Iran*

(Received 02 November 2016; revised manuscript received 08 February 2017; published online 20 February 2017)

Characterization and mechanical behavior was investigated on Cu-Zn-Al shape memory alloy subjected to severe plastic deformation by equal channel angular pressing (ECAP). The microstructure, phase transformation temperatures and morophological features were studied by X-ray diffraction (XRD), scanning electron microscope (SEM), differential scanning calorimetry (DSC) and optical microscope (OM). Homogenous microstructure and grain refinement, which leads to improvement of mechanical properties, was readily achieved by severe plastic deformation (SPD). The XRD results showedtransformation happened from α-phase to martensite phase which induced by the mechanical activated transformation process that has also resulted in the increase of martensite start temperature (M_S) after the ECAP process. The alloy's Vickers hardness increased rapidly from 136 to 217 through the first pass at 400 °C, and then it increased slowly and tended to be stable with increasing of ECAP passes. The yield and compressive strength of specimens increased 242 % and 29 % after ECAP process.

Keywords: Shape memory alloy, Equal channel angular pressing (ECAP), Martensitic transformation, Compressive strength and hardness.

DOI: 10.21272/jnep.9(1).01008 PACS number: 62.20.fg

1. INTRODUCTION

Shape memory alloys (SMA) are a group of smart materials which can be plastically deformed at low temperature, and upon increasing temperatures (to define temperature) or unloading, revert to their primary shape[1]. Ni-Ti (Nitinol) and Cu-based alloys are the two main group of SMAs, which among them the most commercial usage belong to nitinol [2]. The Ni-Ti based SMA's have two important problems, a very strong limitation of transformation temperatures (about 120 °C) while there is a current increasing demand of shape memory alloys to be used as smart materials at higher temperatures (range 200 °C) [3]. On the other hand they are very expensive (100 times more) compares with Cu-based SMA's [4]. Therefore, Cu–based alloys have been used as a preferential alternative to Nitinol for high temperature applications, because they show high thermal stability, a lower cost than Ni-Ti and transformation temperatures as high as 200 °C [5].

Cu-based (Cu-Zn and Cu-Al) shape memory alloys have been studied comprehensively for practical applications because of their low cost, reasonable shape memory and good damping properties and have developed rapidly in recent years. However, these alloys suffer from low ductility and poor mechanical properties which are due to their intrinsic large grain sizes and high elastic anisotropy [6, 7].Cu-based SMAs has been applied gently in different industries like medicine, automotive and aerospace after solving these problems [8].

Cu-Zn based SMAs have been studied less than Cu-Al based SMAs especially in microstructural and mechanical properties in recent years. The M_S of Cu-Zn binary alloys around 40 wt% Zn (38.5-41.5 wt % Zn) is far below room temperature (– 180 °C to – 10 °C) which limits application of this alloy [9]. In order to increase *Ms* (– 180°C to 200 °C), ternary elements such as Al, Ga, Si and Sn are added, the best choice with respect to ductility and grain boundary fracture is Cu-Zn-Al SMAs[10].The Cu-Zn-Al SMA's have been industrially manufactured since 1990 with the chemical composition ranging between (19-30) wt % Zn – (2-6) wt % Al – balance Cu which is the most commonly used compare this with the other Cu-Zn based SMA's [6]. They have not been investigated enough with regard to the influence of the manufacturing technology and microstructure on the shape memory properties. Liu Hai-Xia et al [11], Perkins and Musemg [12], LI and Ansell [13] and Tadaki et al. [14] studied the effect of thermal cycling on Cu-Zn-Al alloys. V. Asanovic and K. Delijic [15] researched the effect of chemical composition on mechanical properties and shape memory capacity of Cu-Zn-Al. Also L. Daroczi et al [16] investigated the effect of hydrostatic pressure on the M_s of Cu-Zn-Al-Mn SMA.

Severe plastic deformation (SPD) is one of the most effective and modern methods for grain refinement of SMAs. Various techniques based on SPD have been developed to produce of ultra-fine grain (UFG) or nanocrystalline (NC) materials including equal-channel angular pressing (ECAP), accumulative roll bonding (ARB), high pressure torsion (HPT), low temperature rolling (LTR) and dynamic plastic deformation (DPD) [17, 18]. Among them ECAP is the most important and useful SPD method for fabricationof bulk UFG and NC materials, because of low cost, convenient design, production of instrument, easy transportation, simple ways for using of machine and versatile processing

* navidbagherpour@gmail.com

techniques [19, 20].

In this paper, the effects of ECAP on the microstructure and mechanical properties of Cu-25 wt % Zn-3.59 wt % Al SMA were investigated.

2. MATERIALS AND METHODS

The Cu-25 wt % Zn-3.59 wt % Al shape memory alloy was prepared by melting elements with industrial purity in an induction furnace and then was founded into metal mold which was chosen to reduce impurities. The alloy was homogenized at 760 °C for 10 h in vacuum furnace and was cooled to room temperature in the furnace. The specimens with dimension of 10 mm × 30 mm were annealed at 800 °C for 2 h. Then the two following heat treatment procedure were applied: quenching in the oil at room temperature and slow cooling in furnace. The initial grain size was measured after annealing which was equal to approximately 162 μm. The ECAP procedure was performed at 400 °C (for the temperature regulation of the samples a coil which was seted around the samples was used as an external heating element) by using a die which was fabricated from a steel tool with two channels intersecting at inner angle of 90° and outer angle of 17.53°. The ram speed was 1 mms^{-1} and oil-graphite was used as lubricant. The samples (denoted by E_0, E_1, E_2 and E_3 which are un-ECAPed, one, two and three times ECAPed) rotated by 180° between each pass. In order to analyze the alloy's microstructure via optical microscope, all specimens were mechanically polished and etchant with composition of 5gr $FeCl_3$ – 10 ml HCl – 100 ml water [21] was used. The SEM observations and chemical analysis were performed by scanning electron microscope technique (Tescan Vega II) which was equipped with energy dispersive X-rays analysis (EDX). The transformation temperatures of the samples were measured under atmospheric pressure by DuPont 2000 DSC Instrument with a scanning rate of 10°C/min in the – 100 °C-100 °C range. The structural and phase analysis of samples were performed by PW 1800 Philips X-ray diffractometer with a graphite monochromator, using CuKα radiation ($\lambda = 1.2405$ Å) by scanning in the $2\theta = 20$-90° range with 0.02° steps. In order to determine the mechanical properties of quenched samples, the microhardness test (reference standard: ASTM E 384-2011, applied force: 10HV) and the compression test (reference standard: ASTM D 695-02a, applied rate: 2 mm/min, diameter and height of samples: 5 mm and 10mm) were performed at room temperature.

3. RESULTS AND DISCUSION

3.1 Microstructure and Phase Study

The parent phases and the martensite plates are revealed by optical microscopic observations of all annealed and quenched specimens, as shown in Fig. 1.

As can be seen in Fig. 1(a) and (b) and with attention to the composition of alloy [22], the annealed and quenched samples have two phases. These phases are α phase (dark region) and β phase (for annealed sample) or martensite phase (for quenched samples), which is observed as a bright region, according to the phase diagram of Cu-Zn-Al and results of SEM point analysis. The phase sizes were reduced significantly after the first pass, and phase refinement was less than the first pass in subsequent passes (Fig. 1(c) and 1(d)).

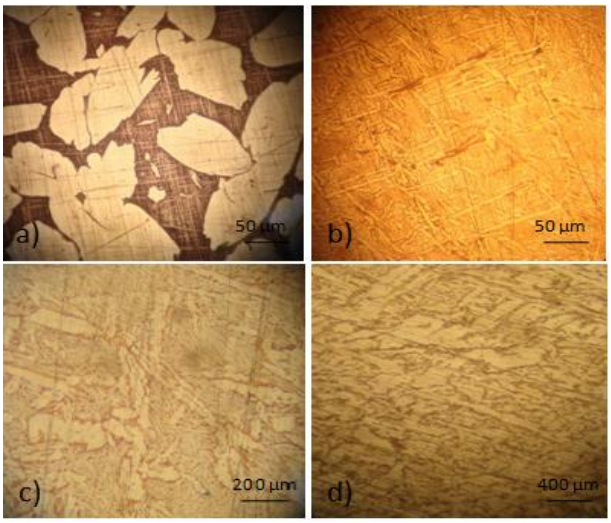

Fig. 1 – Optical microstructures of: (a) initial structure of annealed sample; (b) initial structure of quenched E_0 sample; (c), (d) structure of quenched E_1 and E_3 samples

According to previous results, it is obvious that the first pass is the most effective pass on the microstructure of samples. Fig. 1(d) indicates that the grain size decreased to ultra-fine scale and distribution of phases became more homogenize after the third pass.

Fig. 2 depicts the SEM micrographs of the furnace-cooled (Fig. 2a) and oil-cooled samples (Fig. 2b).

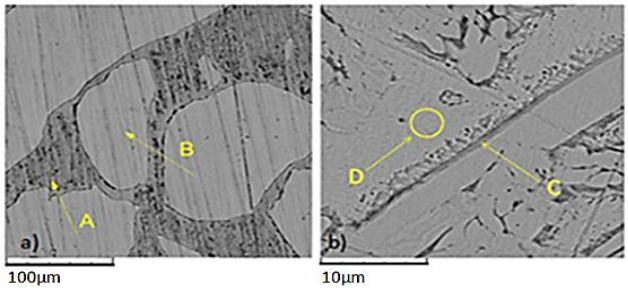

Fig. 2 – The SEM micrographs of: (a) annealed sample; (b) E_0

The EDX analysis was performed to determine the chemical composition of different phases before and after quenching. The EDX results for phases which were indicated in the Fig. 2 are presented in Table 1.

Table 1 – Chemical composition of indicated regions on SEM micrographs by EDX

Specified Points	Wt (%)		
	Cu	Zn	Al
A	71.64	24.23	4.13
B	65.72	27.89	6.39
C	66.91	26.90	6.19
D	71.45	24.34	4.21

Considering the chemical compositions and phase diagram of Cu-Zn-Al, the phases were indicated with A,

B, C and D in Fig. 2 were estimated to be α-phase, β-phase, martensite-phase and α-phase (matrix phase), respectively. The β and martensite phases have nearly the same composition that revealed the β-phase transformed to martensite phase by the quench process.

Quenching Cu-base alloys in water or oil, leads to $\beta \rightarrow M$ phase transformation which is responsible for shape memory properties in these alloys. This type of alloys are delicate to be rapid cooled that makes stabilization of martensite phase and rising of M_S [23].

The size of martensite plates was measured for E_0 and E_3 samples to investigate the effect of ECAP passes on martensitic phase refinement. Fig. 3 presents the average martensite phase sizes before and after the ECAP process.

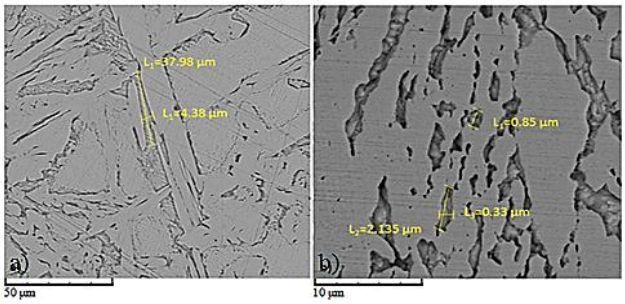

Fig. 3 – The SEM micrographs of samples that show the effect of ECAP on the phase refinement: (a) E_0; (b) E_3

It is evident that the average size of martensite plates was reduced from 20 µm to 1 µm after 3 passes of ECAP (Fig. 3)

In other hand, a remarkable homogenization of martensite distribution was achieved by severe plastic deformation which is obvious in Fig. 4. It is expected that the mechanical properties of alloy experiment significant improvement due to refinement and homogenization of martensite phase which are considered at following discussion.

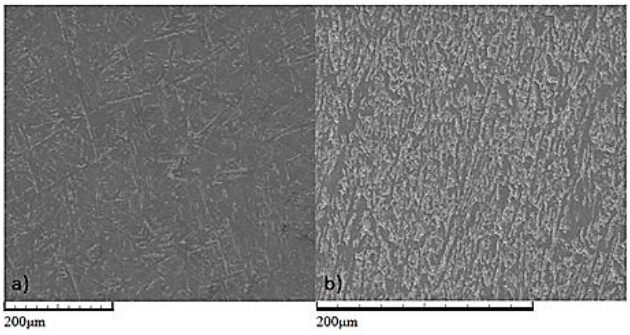

Fig. 4 – Distribution of martensite phase in microstructure of alloy: (a) E_0; (b) E_3

The X-ray diffraction pattern of the samples are delineated at Fig. 5, to confirm the SEM obtained results, and to determine the crystal structure of different phases and the effect of ECAP on microstructure of alloy.

The peaks observed in the profiles are identified as M18R martensite superlattice reflections and α-phase indexed on the monoclinic phase and face centered cubic (FCC) structure, because the alloys were in the martensite /α-phase state at room temperature. Parent phase was also present as a minor component.

M18R is the most unstable structure of martensite phase which makes twin systems in alloy and consequently result in shape memory capability. In shape memory cycle, the alloy with unstable M18R structure, after deformation, returns to primary shape at the austenite phase by rising temperature up to the A_S (austenite start temperature) [24]. M18R with mentioned properties is the most appropriate structure for the alloy which has shape memory property [25]. On the other hand, full shape memory recovery (100 %) could not be expected, because of presence of small quantity of α-phase [15].

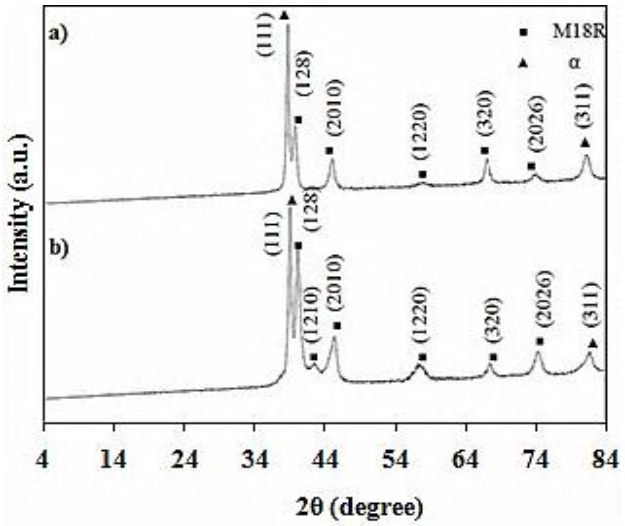

Fig. 5 – X-ray diffraction pattern of the samples: (a) E_0; (b) E_3

Comparison of Fig. 5 (a) and (b) demonstrates that martensite peaks increased by partially transforming of α-phase with FCC structure to martensite phase. A peak which is detectable at $2\theta = 42°$ is likely corresponded to martensite phase with monoclinic structure. As pointed out by Zengin et al. [23], the formation of α-phaseor other precipitates causes the decrease of the transformation temperature by preventing martensite formation, and reduction of the shape memory capacity which is related to the interaction of martensite interfaces with precipitates and defects. From these results it can be said that by increasing of martensite formation, one of the most important effect of SPD on the sample's structure, the increase of Ms is obvious which is detected in DSC results.

This indicates that ECAP improves shape memory properties of alloy by induction of mechanical activated transformation.

Stacking fault energy (SFE) is one of crucial parameters in the cubic-structured materials on the microstructure and plastic deformation after ECAP. By reduction in SFE of alloy, dislocation density decrease which may be attributed to the short-range order or due to the preferential formation of deformation twins [26]. Considering this, more shear bands are operated to help undertake the severe plastic deformation which helps the SPD process. Other than these two common deformation mechanism, dislocation slip and defor-

mation twins, shear bands play more remarkable roles in carrying the shear strain with the decrease of SFE. It is well established that a low SFE strongly facilitates the formation of shear bands. According to these results, it was found that the mechanical behavior of UFG materials can be globally improved by lowering the SFE.

In order to deliberate the SMA behavior of ECAPed alloy, the transformation temperatures which are the key parameters for evaluating the shape memory characteristics are determined by DSC curves (Fig. 6).

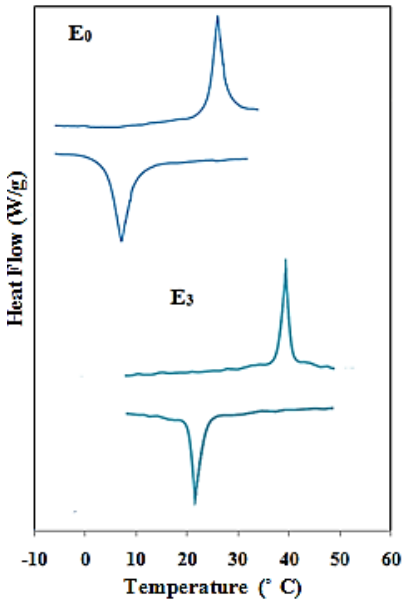

Fig. 6 – DSC curves of the samples with scanning rate of 10 °C/mm

Comparison of phase transformation temperatures of E_0 and E_3 samples which are listed in Table 2 indicates that M_S temperature increased, due to the increase of martensite phase, after three passes of ECAP. This means that the shape memory properties of the alloy improved with grain refinement. These contents emphasize the results which were obtained by X-ray diffraction and shows that the phase transformation behavior of the alloy can be changed by mechanical processing conditions.

Table 2 – Phase transformation temperatures of E_0 and E_3 samples

Sample	Temperature(°C)			
	M_S	M_F	A_S	A_F
E_0	17	10	29	34
E_3	25	20	37	42

This makes better condition of application for the alloy which can be explained by the martensitic phase formation in alloy, caused by rapid cooling and ECAP process, at room temperature. It can be concluded that rapid cooling and SPD have considerable effects on the shape memory property of CuZnAl alloys. In this situation, the alloy requires less temperature variation for phase transformation that makes optimum condition of application.

In order to better reveal the effect of ECAP on phase transformation temperatures, the DSC results of E_0 and E_3 are reviewed comparatively in Fig. 7.

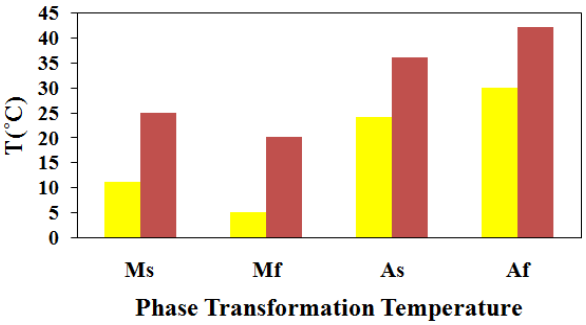

Fig. 7 – Comparison of phase transformation temperatures of E_0 (yellow columns) and E_3 (red columns)

3.2 Mechanical Properties

3.2.1. Hardness

In order to investigate the effect of homogeneous distribution of martensite phase and grain refinement via severe plastic deformation on hardness of alloy, the microhardness test was performed on E_0, E_1, E_2 and E_3. The measured Vickers microhardness of the samples versus the number of passes is shown in Fig. 8.

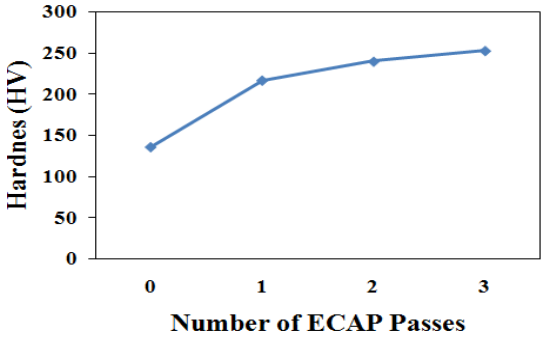

Fig. 8 – Microhardness values of the samples

After 95 % reduction, the crystallite size is about 1 um and it imperecibility decrease by further ECAP.

This corresponds to increase in the Vickers hardness (Hv) and formation of macroscopic shear band.

Although many CuZnAl SMAs reported in the literature show martensitic transformation below room temperature, according to Table 2 the M_S increased up to ambient temperature. With the increasing passes number, magnitude of hardness dramatically increased after the first pass (136 Hv to 217 Hv), but the increment rate of hardness decreased after that. To better compare, an increase of approximately 87 % was observed in magnitude of the hardness after the first pass whereas only 5-10 % increase was seen at subsequent passes.

This situation determines that three passes of ECAP for achieving grain refinement and homogeneous distribution of martensite phase were suitable.

3.2.2. Compression Behavior

Fig. 9 shows the compressive engineering stress-strain of samples which were processed from 1- to 3-

pass ECAP. The mechanical properties, including yield stress (*Ys*), compressive strength (*Cs*) and elongation to fracture (E_f), as a function of the number of ECAP passes are summarized in Fig. 9 to evaluate the effect of homogeneous distribution of martensite phase and grain refinement on the compressive behavior of alloy.

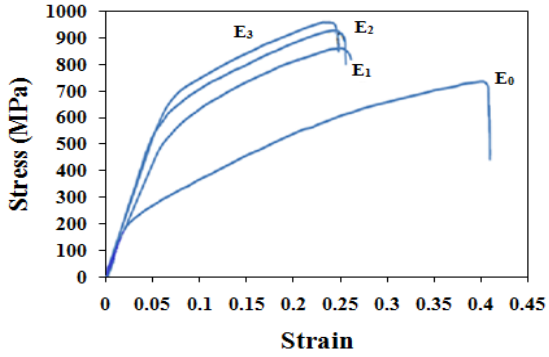

Fig. 9 – Stress-strain curves of quenched samples: E_0, E_1, E_2 and E_3

As can be seen, significant variations in magnitudes were obtained for the first pass and then gradual changes were received for subsequent passes.

It is obvious that yield and compression strength increased with enhancing number of ECAP passes which is caused by the homogenized distribution of rough martensite phase in the α-phase (soft phase) and grain refinement but the magnitude of elongation decreased which was almost constant after the first pass (Fig. 10).

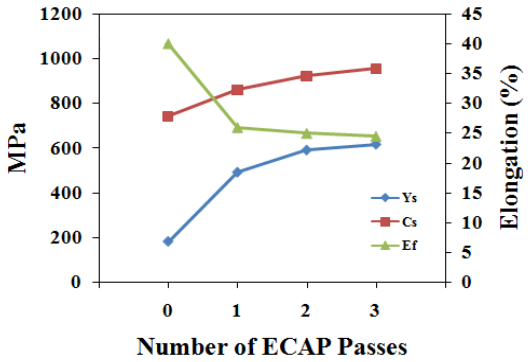

Fig. 10 – Mechanical properties of samples before and after ECAP, including *Ys*, *Cs* and E_f

However, the E_f of the ECAPed samples showed a slight decrease with the number of passes which can be attributed to a smaller increase in the strain hardening rate Θ as the stress increases[11](Fig. 10).

The yield and compressive strength significantly increased 172 % and 16 % at first pass, respectively. The increasing rate was reduced after the first pass. A similar trend was observed in the hardness behavior, so that total increasing of magnitudes are 242 % for yield strength and 29 % for compressive strength.

4. CONCLUSIONS

The SMA specimens with chemical composition of Cu-25 wt % Zn-3.59 wt % Al were casted and heat treated. To achieve a homogenous and stable structure and to tailor the mechanical properties, samples were subjected to ECAP including multiple steps of severe plastic deformation. The prominent conclusions can be drawn as follows:

• Microstructure and phase analysis by OM, XRD and SEM was indicated that the alloy has two phases: α-phase (FCC structure) and β-phase (BCC structure) which transformed to martensite phase (monoclinic structure) after quenching.

• The martensite phase refinement occurred after three passes of ECAP and the size of martensite plates was reduced from 20 μm to 1 μm.

• Distribution of martensite phase was homogenized after the third pass which is the most important factor for improving of mechanical properties of the alloy.

• Partially transformation of α-phase to martensite phase and formation of a peak at $2\theta = 42°$ after three passes of ECAP which might be the martensite phase showed shape memory properties of alloy were boosted with SPD technique that was induced by mechanical activated transformation process.

• M_S increased after severe plastic deformation that results in more applications and optimization of working conditions of the alloy.

• Homogenous distribution of martensite phase and refined grain size improved mechanical properties like hardness, yield, compressive strength of the alloy significantly and the first pass was the most effective pass on mechanical properties.

• Improvement of more than three times in yield strength and more than 200 MPa in ultimate strength was seen in ECAPed samples compared with un-ECAPed sample. On the other hand, the elongation of the alloys decreased about 15 % during the ECAP process.

REFERENCES

1. *Properties and selection: Nonferrous alloys and special-purpose materials* Steven:*ASM handbook* (Ed. R. Lampman, Th.B. Zorc) (United States of America: ASM International: 1990).
2. M.V. Gandhi, B.S. Thompson, *Adv. Mater.* **5**, 313 (2004).
3. H. Ghourchibeigy, A. Shokuhfar, M.S. Haghighat Nia, F. Arabi, M. Arjmand, *Proc. Conf. Nanothechnology and Biosensors* **2**, 72 (Singapore: IACSIT Press: 2010).
4. S. Eucken, *Mater. Manuf. Process.* **7**, 201 (1992).
5. P. Haasen, *Wiley-VCH.* **5**, 339 (1991).
6. I. Hopulele, S. Istrate, S. Stanciu, G.H. Calugaru, *J. Optoelectron. Adv. M.* **6**, 277 (2004).
7. X. Balandraud, D. Delpueyo, M. Grediac, G. Zanzotto, *Acta Mater.* **58**, 4559 (2010).
8. W.M. Huang, Z. Ding, C.C. Wang, J. Wei, Y. Zhao, H. Purnawal, *Mater. Today.* **13**, 54 (2010).
9. H. Pops, T.B. Massalski, *Acta Metall.* **15**, 1770 (1967).
10. K. Otsuka, C.M. Wayman, *Shape memory materials* (United Kingdom: The Press Syndicate of University of Cambridge: 1999).
11. L. Hai-Xia, Si. Nai-Chao, X. Gui-Fang, *Trans. Nonferrous Met. Soc. China.* **16**, 1402 (2006).

12. J. Perkins, W.E. Museing, *Metall. Trans. A* **14**, 33 (1983).
13. J.C. Li, G.S. Ansell, *Metall. Trans. A* **14**, 1293 (1983).
14. T. Tadaki, M. Tamkamori, K. Shimizu, *Trans. JIM.* **28(2)**, 120 (1987).
15. V. Asanović, K. Delijić, *Metalurgija* **13**, 59 (2007).
16. L. Daro´Czi, D.L. Beke, C. Lexcellent, V. Mertinger, *Scripta Mater*. **43**, 691 (2000).
17. R.Z. Valiev, R.K. Islamgaliev, I.V. Alexandrov, *Prog. Mater. Sci*. **45**, 103 (2000).
18. B. Verlinden, *Metalurgija* **11**, 165 (2005).
19. J. Macheret, G.E. Kort, T.M. Lillo, A.D. Watkins, *Equal Channel Angular Extrusion*, Report INEEL/EXT-99-00459, Home of Science and Engineering Solutions, Idaho National Engineering and Environmental Laboratory, USA, 1-65, (1999).
20. M. Greger, R. Kocich, L. Cizek, L.A. Dobrzañski, M. Widomská, *Mater. Sci. Eng*. **28**, 709 (2007).
21. *Metallography and microstructures: ASM Handbook* (Ed. G.F. Vander Voolt) (Materials park, OH, United State of America: ASM International: 2004).
22. U. Borggren, M. Salleby, *J. Phase Equilib*. **24**, 110 (2004).
23. R. Zengin, N. Kayal, *Acta. Phys. Pol. A* **118**, 619 (2010).
24. A. Cuniberti, R. Romero, M. Stipcich, *J. Alloy. Compd.* **472**, 162 (2009).
25. F.C. Bubani, M. Sade, F. Lovey, *Mater. Sci. Eng. A* **543**, 88 (2012).
26. S. Qu, X.H. An, H.J. Yang, C.X. Huang, G. Yang, Q.S. Zang, Z.G. Wang, S.D. Wua, Z.F. Zhang, *Acta Mater.* **57**, 1586 (2009).